Published in final edited form as:
Bioconjug Chem. 2010 July 21; 21(7): 1206–1215. doi:10.1021/bc100018n.

Liposomal Cu-64 labeling method using bifunctional chelators: polyethylene glycol spacer and chelator effects

Jai Woong Seo, **Lisa M. Mahakian**, **Azadeh Kheirolomoom**, **Hua Zhang**, **Claude F. Meares**[1], **Riccardo Ferdani**[2], **Carolyn J. Anderson**[2], and **Katherine W. Ferrara**[*]

Department of Biomedical Engineering, University of California, Davis, CA 95616

[1]Department of Chemistry, University of California, Davis, CA 95616

[2]Mallinckrodt Institute of Radiology, Washington University School of Medicine, St. Louis, MO 63110

Abstract

Two bifunctional Cu-64 chelators (BFCs), (6-(6-(3-(2-pyridyldithio)propionamido)hexanamido)benzyl)-1,4,8,11-tetraazacyclotetradecane- 1,4,8,11-tetraacetic acid (TETA-PDP) and 4-(2-(2-pyridyldithioethyl)ethanamido)-11-carboxymethyl-1,4,8,11-tetraazabicyclo(6.6.2)hexadecane (CB-TE2A-PDEA), were synthesized and conjugated to long circulating liposomes (LCLs) via attachment to a maleimide lipid. An *in vitro* stability assay of ^{64}Cu-TETA, ^{64}Cu-TETA-PEG2k, and ^{64}Cu-CB-TE2A-PEG2k liposomes showed that more than 86% of the radioactivity remains associated with the liposomal fraction after 48 hours of incubation with mouse serum. The *in vivo* time activity curves (TAC) for the three liposomal formulations showed that ~50% of the radioactivity cleared from the blood pool in 16 - 18 hours. As expected, the *in vivo* biodistribution and TAC data obtained at 48 hours demonstrate that the clearance of radioactivity from the liver slows with the incorporation of a polyethylene glycol-2k (PEG2k) brush. Our data suggest that ^{64}Cu-TETA and ^{64}Cu-CB-TE2A are similarly stable in the blood pool and accumulation of radioactivity in the liver and spleen is not related to the stability of Cu-64 chelator complex; however clearance of Cu-64 from the liver and spleen are faster when injected as ^{64}Cu-TETA-chelated liposomes rather than ^{64}Cu-CB-TE2A-chelated liposomes.

Keywords

liposome; Cu-64; PET; TETA; CB-TE2A; liposomal stability in blood; spleen and liver

Introduction

Liposomes, spherical vehicles composed of lipid bilayer with aqueous interior, have been investigated more than 40 years as a promising drug carrier (1-3). When coated by polyethylene glycol, liposomal circulation time in blood increased with a decrease in reticuloendothelial system (RES) uptake (4-6). Currently, 90-100 nm diameter liposomes entrapping anticancer or antifungal drugs are approved and used for passively targeting the relatively leaky vasculature of tumors (7,8). Advanced liposomal technology exploits peptide (9,10), antibody (11,12), and small molecule ligands (13,14) by attaching these ligands on the surface of liposomes to maximize the retention at the target site. In addition,

[*]To whom correspondence should be addressed: Prof. Katherine W. Ferrara Dept. of Biomedical Engineering 451 East Health Sciences Drive University of California, Davis Davis, CA 95616 PHONE 530-754-9436 FAX (530)754-5739 kwferrara@ucdavis.edu.

triggered drug release by ultrasound (15,16) or a laser (17,18) and in a low pH environment (19) has been explored for local delivery.

Non-invasive imaging techniques using SPECT and PET have been developed to evaluate the pharmacokinetics and biodistribution of liposomes *in vivo* (20-22). Previous studies have utilized liposomes with radionuclides such as technetium-99m (23-27), gallium-67 (28), and indium-111 (29,30) for single photon emission computed tomography (SPECT) and fluorine-18 (31-33), iodine-124 (34), oxygen-15 (35), and copper-64 (36) for positron emission tomography (PET), where radionuclides were applied with three distinct schemes involving entrapment, insertion, and chelation. In the entrapment method, radionuclides such as indium-111 ($t_{1/2}$ = 2.8 days), gallium-67 ($t_{1/2}$ = 3.3 days), and technetium-99m ($t_{1/2}$ = 6.01 h), were coordinated with membrane permeable lipophilic chelators and loaded into the aqueous liposomal core with a change to a hydrophilic chelator (25,26,28,30). As an insertion method, radiolabeled lipids, 3-[^{18}F]fluoro-1,2-dipalmitoylglycerol ([^{18}F]-FDP) or [^{18}F]-labeled amphiphilic lipids, were incorporated into the liposomal bilayer (31,33). Surface chelation methods, the most convenient method, were also developed with technetium-99m or copper-64 ($t_{1/2}$ = 12.7 h) by covalently attaching the chelator on the surface of the liposome (27,36) or conjugating ^{18}F-labelled PEG-acetylene with an azide group on the liposome via a “click” reaction (37).

The previous labeling approaches were focused on obtaining a stable conjugation of a radionuclide and liposome to quantify the liposomal activity in target tissues over days to weeks without the radionuclide undergoing metabolism or becoming de-complexed. We previously developed a liposomal Cu-64 labeling method using 6-[*p*-(bromoacetamido)benzyl]-1,4,8,11-tetraazacyclotetradecane-*N*,*N*′,*N*″,*N*‴-tetraacetic acid (BAT) conjugated lipid (6-BAT-lipid) and successfully measured the liposomal circulation time in blood over 48 hours (36). However, liposomes with high molar concentrations of peptide have shown a lower radiolabeling yield. CB-TE2A, which forms a highly stable complex with Cu-64, has not previously been explored in a liposomal study using a post-labeling method because the chelation of Cu-64 should be performed at a temperature above 80 °C which may affect liposomal stability due to the intrinsic transition temperature of the liposome (38,39).

Recent studies of targeted nanoparticles combine antibodies, peptides, small molecules and polymers on the surface to optimize and personalize targeting (9-14). For this reason, it is important to optimize radiochemistry techniques for specific surface architectures; and therefore alternative post-labeling methods and CB-TE2A are explored. Herein, we developed and evaluated a Cu-64 labeling method using a maleimide lipid and bifunctional chelator (BFC). Stability *in vitro* and *in vivo* is then compared for liposomes labeled with TETA-PDP and CB-TE2A-PDEA, and with varied spacer lengths between the lipid and chelator.

Materials

HSPC, DSPE-PEG2k-maleimide, cholesterol, DSPE-PEG2k-OMe, were purchased from Avanti Polar Lipids (Alabaster, AL) and DSPE-maleimide was purchased from NOF America Corporation (White Plains, NY). Sulfo-LC-SPDP (sulfosuccinimidyl 6-[3′(2-pyridyldithio)-propionamido]hexanoate) was purchased from Thermo scientific (Rockford, IL). S-(2-Aminoethyl)dithio-2-pyridine hydrochloride was purchased from Toronto Research Chemicals (North York, ON). Solvents and other agents were all of analytical purity and purchased from Sigma-Aldrich (Milwaukee, WI) and VWR (Brisbane, CA). $^{64}CuCl_2$ was purchased from Isotrace (St. Louis, MO) under a protocol controlled by

the University of California, Davis. PBS was purchased from Invitrogen Corporation (Carlsbad, CA). Mouse serum was purchased from Innovative research (Novi, MI).

Experimental Section

Synthesis of TETA-PDP (2)

(6-(6-(3-(2-Pyridyldithio)propionamido)hexanamido)benzyl)-1,4,8,11-tetraazacyclotetradecane- 1,4,8,11-tetraacetic acid (TETA-PDP, **2**) was synthesized from aminobenzyl-TETA (1) based on a previously reported method (40,41). To a solution of **1** (18 mg, 34 μmol) in DI water (2 mL, pH 7) was added sulfosuccinimidyl-6-[3′(2-pyridyldithio)-propionamido]hexanoate (22 mg, 42 μmol). The mixture was stirred at room temperature for 4 hours. Reaction progress was monitored by a semi-preparative HPLC (column: Jupiter 10μ proteo, 250 × 10 mm; flow rate: 3 mL/min; eluent: A - MeOH, B - 0.05% TFA in triple-distilled water; gradient: 0-15 min (40 - 80% A), 15-30 min (80 - 100% A)) and retention time was 11 min. Coupled product **2** was isolated by preparative HPLC (column: Jupiter 10μ, 250 × 21.2 mm; flow rate: 10 mL/min; eluent: A - MeOH, B - 0.05% TFA in triple-distilled water; gradient: 0-15 min (40 - 80% A), 15-30 min (80-100% A); retention time: 13.3 ± 0.36 min) and lyophilized as a white solid (25 mg, 87%). ^{1}H NMR (500 MHz, D_2O): 8.48 (d, *J* = 5.5 Hz, 1H), 8.12 (t, *J* = 8.0 Hz, 1H), 7.91 (d, J = 8.5 Hz, 1H), 7.55 (t, *J* = 6.0 Hz, 1H), 7.36 (d, *J* = 7.5 Hz, 2H), 7.30 (d, *J* = 8.0 Hz, 2H), 3.35-3.65 (m, 12H), .2.95-3.32 (m, 16H), 2.61 (t, *J* = 6.5 Hz, 2H), 2.55-2.45 (m, 3H), 2.08 (bs, 1H), 1.78 (bs, 1H), 1.73 (m, 2H), 1.54 (m, 2H), 1.39 (m, 2H); MS (ESI) m/z 848.4 ($M+H^+$).

Synthesis of CB-TE2A-PDEA (4)

4-(2-(2-Pyridyldithioethyl)ethanamido)-11-carboxymethyl-1,4,8,11-tetraazabicyclo(6.6.2)hexadecane (CB-TE2A-PDEA, **4**) was synthesized from CB-TE2A (**3**) synthesized as in (42,43). To a solution of **3** (68 mg, 0.1 mmol) in DMF (4 mL) was added 3-(dimethylamino)propyl)ethyl carbodiimide hydrochloride (EDCI·HCl, 9.6 mg, 50 μmmol), *N*-hydroxybenzotriazole (HOBt, 8.1 mg, 60 μmol) and *N*,*N*-diisopropylethylamine (DIPEA, 52 μL, 0.3 mmol). After stirring for 30 min at room temperature, *S*-(2-aminoethyl)dithio-2-pyridine hydrochloride (11 mg, 50 μmol) was added and the reaction mixture was stirred overnight. The solvent was removed under high vacuum and residual oil was injected into the preparative HPLC after dilution of oil with a 0.05% TFA solution (column: Jupiter 10μ, 250 × 21.2 mm; flow rate: 10 mL/min; eluent: A - acetonitrile, B - 0.05% TFA in 3rd distilled water; gradient: 0-15 min (20 - 25% A), 15-30 min (25 - 90% A); retention time: 9.3 ± 0.35 min). The collected product fraction was lyophilized and **4** obtained as a white powder (19 mg, 74%), ^{1}H NMR (500 MHz, D_2O): 8.58 (d, *J* = 5.0 Hz, 1H), 8.23 (t, *J* = 8.5 Hz, 1H), 8.13 (d, *J* = 8.5 Hz, 1H), 7.64 (t, *J* = 6.5 Hz, 1H), 4.22 (d, *J* = 15.5 Hz, 1H), 4.02 (d, *J* = 16.0 Hz, 1H), 3.76-3.62 (m, 3H), 3.62-3.51 (m, 2H), 3.50-3.34 (m, 4H), 3.25-2.90 (m, 15H), 2.75 (bd, *J* = 13.5 Hz, 1H), 2.75 (dd, *J* = 13.5, 2.0 Hz, 1H), 2.45-2.31 (m, 2H), 1.75 (t, *J* = 16.5 Hz, 2H); MS (ESI) m/z 511.5 ($M+H^+$, 100).

HPLC analysis of Cu-64 chelation with CB-TE2A-PDEA

A few micro-liters of $^{64}CuCl_2$ were buffered with 0.1 M ammonium citrate (100 μL). CB-TE2A-PDE (1 mM, 2 μL) dissolved in ammonium citrate buffer (0.1 M, pH 5.5), was added into a buffered $^{64}CuCl_2$ solution and the mixture was incubated at 85 °C. Samples for HPLC analysis were acquired at 0, 30, and 60 min and kept in an ice-bath until injected to the HPLC. Freshly prepared TCEP (10 mM, 2 μL) in PBS was then added and the mixture was held at room temperature for 10 min and applied to an HPLC column (Jupiter: C12, 250 × 4.6 mm, flow rate: 1 ml/min, eluent - A: 0.5% TFA in deionized water, B: 0.5% TFA in acetonitrile, 0 - 10 min (10 - 20% B), 10 - 20 min (20 - 100% B), 20 - 24 min (100% B), 24 - 25 min (100 - 10% B)).

Preparation of maleimide liposomes

Commercially-available lipids (10 mg of HSPC, Cholesterol, DSPE-PEG2k-OMe, and 1 mol% DSPE-PEG2k-maleimde or DSPE-maleimide) in chloroform were mixed in a test tube. Chloroform was evaporated by a gentle stream of nitrogen with a vortex. After drying overnight in a lyophilizer, lipids were suspended in PBS (1X). The lipid solution was incubated at 60 °C for 5 min, drawn into the 1 mL syringe, and extruded at 60°C by a mini extruder unit with 100 nm filters. Immediately after extrusion, the size was measured using a NICOMP 380 ZLS (Particle Sizing Systems, CA) and liposomes were labeled with Cu-64 labeled bifunctional chelators. The average of liposomal diameter was 123.6 ± 13.0 nm.

Labeling of maleimide liposomes with BFCs

All labeling procedures were controlled under a protocol of the University of California, Davis. $^{64}CuCl_2$ (0.55 - 5 mCi, [18.5 -185 MBq]) was buffered with 0.1 M ammonium citrate (100 μL). TETA-PDP or CB-TE2A-PDEA (1 mM, 10 ~ 2 μL) in an ammonium citrate buffer (0.1 M, pH 5.5) was added into a $^{64}CuCl_2$ solution, which was incubated for 40 min at 30 °C or 1.5 hours at 85 °C, respectively. The reaction progress was monitored by radio TLC (silica backed plate, eluent-10% (w/w) ammonium acetate and methanol (1:1, v/v)) or radio HPLC. After the addition of 10 times excess of 0.1 M tris(2-carboxylethyl)phosphine hydrochloride (TCEP·HCl) dissolved in PBS, the solution was incubated for 5 min at room temperature. Freshly prepared maleimide liposomes (10, 5, 2.5, and 1 mg) in PBS (0.4 mL) were added to the reduced bifunctional chelator mixture. The pH was adjusted with 5.6% (v) ammonium hydroxide solution and the liposomal mixture was incubated for 40 min at 30 °C. After cooling of the liposomal mixture, unreacted maleimide on the surface of the liposomes was quenched by an excess (maleimide : ethanethiol = 1:10, mol/mol) of freshly prepared 0.1 M ethanethiol solution by incubating for 10 min. Lastly, non-specific binding of Cu-64 was removed by 0.1 M EDTA (20 μL) incubation for 5-10 min. Liposomes were purified by size exclusion chromatography with PBS.

In Vitro Stability Test

^{64}Cu-labeled liposomes (^{64}Cu-TETA, ^{64}Cu-TETA-PEG2k, and ^{64}Cu-CB-TE2A-PEG2k liposomes, 1 mg, 10.1 – 12.28 MBq) were added to 0.5 mL of mouse serum and PBS and the mixture was incubated for 48 hours at 37 °C. After cooling, a portion of the liposomal serum mixture (100 μL) was hand-loaded onto a pre-conditioned sephachryl-300HR (GE Healthcare, NJ) packed column (15 mm I.D, 250 mm height) and separated with PBS at 2 psi. Fractions (1.5 mL/fraction) were collected into test tubes, and the radioactivity was measured with the 1470 Automatic Gamma Counter (Perkin-Elmer Life Sciences, MA). After the radioactive decay, the absorbance of all fractions was measured at 280 nm. The radio TLC assay was run on aluminum-backed silica gel sheets (silica gel 60 F254, EMD, NJ), developed with chloroform/methanol/H_2O (50:40:6, v/v/v) and recorded by a radio-TLC Imaging Scanner (Bioscan, NW).

Biodistribution Study

All animal studies were conducted under a protocol approved by the University of California, Davis Animal Use and Care Committee. A total of 13 animals (female FVB mice, 12-19 weeks, 25-30 g, Charles River, MA) were examined over the course of this study. For each image, four or five mice per group were anesthetized with 3.5% isoflurane and maintained at 2.0 - 2.5%. ^{64}Cu-TETA liposomes (38 ± 0.7 mg/kg, 313 ± 19 μCi [11.58 ± 0.70 MBq]/animal), ^{64}Cu-TETA-PEG2k liposomes, (43 ± 6.7 mg/kg, 332 ± 55 μCi [12.28 ± 2.03 MBq]/animal), and ^{64}Cu-CB-TE2A-PEG2k liposomes (34 ± 1.6 mg/kg, 272 ± 9.2 μCi [10.06 ± 0.34 MBq]/animal) in PBS (pH 7.4) were administered to the mice on a PET scanner bed by catheterized tail vein injection. After scanning over 48 hours, the mice were

euthanized by cervical dislocation, and organs of interest were harvested and weighed. Radioactivity was measured using a 1470 Automatic Gamma Counter.

PET Scans and Time-Activity Curves (TAC)

Two mice were placed on one bed and each set of PET scans was conducted with the microPET Focus (Concorde Microsystems, Inc., TN) over 30 min. Mice were scanned at an initial time point (t = 0), and 6, 18, 28, and 48 hours. Filtered backprojection (FBP) reconstruction was obtained with ASIPro software (CTI Molecular Imaging). TACs were obtained with region-of-interest (ROI) analysis using ASIPro software and expressed as the percentage of injected dose per cubic centimeter (%ID/cc).

Statistical analysis

Prism (GraphPad software Inc., San Diego, CA) was used for statistical analysis. One phase exponential blood clearance curves were generated via a curve fit. The data analysis was performed using one-way analysis of variance (ANOVA).

RESULTS

Synthesis of TETA-PDP (2)

Aminobenzyl TETA **1**, precursor of TETA-PDP, was achieved in 5 steps from 4-nitrobenzyl bromide as previously reported (40,41). Critical steps in determining the yield were cyclization, where the resulting yield was 40% with *N*,*N*-bis(2-aminoethyl)-1.3-propanediamine, and alkylation where the resulting yield was 41% with benzylbromoacetate. To reduce the contamination from trace metals, aminobenzyl TETA **1** was coupled with sulfosuccinimidyl-6-[3′-(2-pyridyldithio)propionamido]hexanoate in distilled water at pH 7 (scheme). The product was isolated by preparative HPLC with retention time on average 13.3 min and overall synthesis yield was 10%. The final product was validated by ^{1}H NMR spectral analysis and electrospray ionisation-mass spectrometry as a positive mode. A single charged peak (20%) at 848 and a doubly-charged peak (100%) at 425 were detected.

Synthesis of CB-TE2A-PDEA (4)

A half equivalent of S-(2-aminoethyl)dithio-2-pyridine hydrochloride and CB-TE2A was treated with HOBt, EDCI, and DIPEA in DMF to obtain the carboxylic acid-coupled product (scheme). DMF was removed under high vacuum to achieve a consistent retention time of 9.3 min on preparative HPLC. Lyophilization of the product fractions yielded 74% CB-TE2A-PDEA. The product was also validated by ^{1}H NMR spectral analysis and electrospray ionization-mass spectrometry in a positive mode. A single charged peak was detected at 511 (100%).

Radio HPLC analysis of Cu-64 incorporation into CB-TE2A-PDEA and formation of active sulfhydryl group

Incorporation of Cu-64 with TETA is performed at room temperature within one hour. On the other hand, CB-TE2A requires heating (> 80 °C) for incorporation of Cu-64. First, we evaluated the stability of CB-TE2A-PDEA under the chelation conditions at 85 °C. Freshly prepared 2 nmol of 1 mM CB-TE2A-PDEA **4** in ammonium acetate buffer (pH 5.5, 100 μL) was incubated with a few hundred μCi of Cu-64 at 85 °C. The reaction progress and decomposition of Cu-64 incorporated BFC were monitored by HPLC analysis. After the addition of $^{64}CuCl_2$ into the CB-TE2A-PDEA solution, the radiochromatogram showed only the Cu-64 peak eluted at 3 min (**a**, figure 2). After incubation for 30 min and 60 min, 69% and 96% of the radioactivity was observed with a retention time of 15 min, respectively (**b**

and **c**, figure 2), which indicated that Cu-64 was completely incorporated into CB-TE2A-PDEA without decomposition. After the Cu-64 chelation, ^{64}Cu-CB-TE2A-PDEA solution was cooled to room temperature for 10 min and the addition of a ten times excess amount of TCEP (10 mM, 2 μL) as a reducing reagent selectively cleaved the disulfide bond (44). Incubation for 10 minutes converted all Cu-64-incorporated-CB-TE2A-PDEA into the peak at 8 min. Thus, the pyridyldithiol **6** was rapidly reduced to the sulfhydryl-group **7** (**d**, figure 2) with more than 99% yield, which was confirmed by the conversion of retention time of **6** to **7**.

BFC conjugation study with maleimide liposome

Liposomes (average diameter: 119 ± 12 nm) were prepared from HSPC, DSPE-PEG2k-OMe, cholesterol, and DSPE-maleimide (molar ratio 55/5/39/1) and HSPC, DSPE-PEG2k-OMe, cholesterol, and DSPE-PEG2k-maleimide (molar ration 56/4/39/1) (figure 3) as described in the experimental procedure (figure 7). The incorporation of Cu-64 (0.2 - 1 mCi [7.4 - 37 MBq]) into TETA-PDP **2** (2 nmol) at 30 °C was successful (>99%), which was confirmed by the R_f value of radio TLC ($^{64}CuCl_2$: R_f 0, ^{64}Cu-TETA-PDP: R_f 0.45). Treatment by TCEP (10 eq/TETA-PDP), which reduces a disulfide over a wide pH range (45), converted pyridyldithiol **8** to the sulfhydryl compound **9** with more than 99% yield within 10 min (data not shown but similar to figure 2). To increase the nucleophilicity of the thiols, the pH was adjusted to 7.0-7.5. The conjugation yield of ^{64}Cu-TETA-thiol **9** was assessed with 0.5, 1.25, and 2.5 mg of maleimide liposomes which have 7, 17, 35, and 70 nmol of maleimide on the surface of liposome, respectively. The corresponding liposomal conjugation yields were 16 ± 2%, 43 ± 14%, 91 ± 3%, and 93 ± 3% (n=4) for 1 mol% maleimide liposomes, and 20 ± 4 %, 47 ± 17%, , 92 ± 3%, and 94 ± 3% (n=4) for 1 mol% maleimide-PEG2k-liposomes (figure 5). The radiochemical purity checked by the separated liposomal fraction was more than 99% on radio TLC. The specific activity of Cu-64 labeled liposomes in this in vivo study was 20.8 ± 1.6 mCi/μmol maleimide lipid.

In Vitro Stability Test

The *in vitro* stability of BFC conjugated maleimide liposomes was assessed with ^{64}Cu-TETA, ^{64}Cu-TETA-PEG2k, and ^{64}Cu-CB-TE2A-PEG2k liposomes (each 1 mg) in PBS/mouse serum (1/1, v/v) after 48 hour incubation at 37 °C. After size exclusion chromatography (n=3), we obtained 84 ± 2 % of the total radioactivity in 50 fractions (75 mL) from all liposomes. Liposomal fractions eluted from fraction 8 to 15 contain 89% (^{64}Cu-TETA liposomes), 86% (^{64}Cu-TETA-PEG2k liposomes), and 86% (^{64}Cu-CB-TE2A-PEG2k liposomes) of total eluted radioactivity (figure 6). Radiochemical purity, monitored by radio TLC, of each liposomal fraction was more than 98%.

In vivo PET images and Time-Activity Curves (TAC)

In vivo imaging with ^{64}Cu-BFC-labeled liposomes from 30-min scans at 0, 6, 18, and 28 h after intravenous injection demonstrated long circulation of the ^{64}Cu-TETA liposomes (1.0 mg, 313 ± 19 μCi [11.58 ± 0.70 MBq]), ^{64}Cu-TETA-PEG2k liposomes (1.2 mg, 332 ± 56 μCi [12.28 ± 2.03 MBq]), and ^{64}Cu-CB-TE2A-PEG2k liposomes (1.0 mg, 272 ± 9.2 μCi [10.06 ± 0.34 MBq]). Liposomal activity was high in the blood pool from 0 to 6 h and slowly cleared out through the reticuloendothelial system. Time activity curves (TAC) corresponding to blood, liver, and spleen are shown in Figure 8. For ^{64}Cu-TETA liposomes, radioactivity in the blood pool decreased to 41 ± 1.2%, 34 ± 1.6%, 20 ± 0.5%, 13 ± 1.0%, and 8.4 ± 0.6%ID/cc at 30 min, 6, 18, 28, and 48 h, respectively (figure 8b). At the same time points, with ^{64}Cu-TETA-PEG2k liposomes, the radioactivity in the blood pool was 41 ± 3.8%, 31 ± 3.3%, 20 ± 2.0%, 13 ± 2.3%, and 7.6 ± 0.6 %ID/cc, for ^{64}Cu-CB-TE2A-PEG2k liposomes, 39 ± 1.1%, 28 ± 2.3%, 18 ± 2.1%, 11 ± 1.0%, and 6.4 ± 1.6 %ID/cc at 30 min, 6, 18, 28, and 48 h, respectively (figure 8b). Exponential curve-fitting of three

liposomal formulations showed one phase exponential clearance from the blood pool. TAC data obtained from the blood pool was simulated with one phase exponential decay as shown in Table 2.

For the three liposomal preparations, estimated radioactivity in the liver was 10.5 ± 0.8%, 13.3 ± 0.6%, 12.1 ± 0.9%, 8.7 ± 0.1%, and 6.7 ± 0.2 %ID/cc (^{64}Cu-TETA liposomes), 8.1 ± 1.5%, 14.3 ± 1.0%, 15.1 ± 0.9%, 13.7 ± 1.3%, and 11.0 ± 0.8 %ID/cc (^{64}Cu-TETA-PEG2k liposomes), and 7.4 ± 0.9%, 13.5 ± 2.0%, 16.5 ± 2.2, 15.4 ± 2.0%, and 15.7 ± 1.7 %ID/cc (^{64}Cu-CB-TE2A-PEG2k liposomes) at 30 min, 6, 18, 28, and 48 h, respectively (figure 8c). Estimated radioactivity in the spleen was 6.0 ± 1.7%, 8.1 ± 4.1%, 8.1 ± 1.0%, 4.8 ± 1.3%, and 4.2 ± 0.9 %ID/cc (^{64}Cu-TETA liposomes), 7.5 ± 0.8%, 9.6 ± 1.2%, 10.2 ± 2.1%, 9.4 ± 2.4%, and 8.3 ± 2.0 %ID/cc (^{64}Cu-TETA-PEG2k- liposomes), and 6.9 ± 0.6%, 10.8 ± 1.3%, 14.8 ± 3.6, 13.2 ± 4.5%, and 10.4 ± 2.7 %ID/cc (^{64}Cu-CB-TE2A-PEG2k liposomes) at 30 min, 6, 18, 28, and 48 h, respectively (figure 8d).

Biodistribution

The biodistribution at 48 h confirmed the TAC estimates (Table 1). There was no significant difference in blood radioactivity (8.71 ± 0.38%, 8.35 ± 1.10%, and 6.85 ± 1.66 %ID/g) at 48 hours after administration of ^{64}Cu-TETA liposomes, ^{64}Cu-TETA-PEG2k liposomes and ^{64}Cu-CB-TE2A-PEG2k liposomes, respectively. For ^{64}Cu-TETA liposome-injected mice, radioactivity in the liver (6.88 ± 0.96 %ID/g) and spleen (12.26 ± 0.70 %ID/g) was significantly lower than the liver (15.2±1.23 %ID/g, 22.9±4.42 %ID/g) and spleen (20.3 ± 2.49 %ID/g, 30.4 ± 5.25 %ID/g) of ^{64}Cu-TETA-PEG2k and ^{64}Cu-CB-TE2A-PEG2k liposome-injected mice, respectively. Other organs showed a similar biodistribution for the three liposomal formulations (Table 1).

DISCUSSION

The first aim of this study was to develop a liposomal conjugation method using a Cu-64 and thiol reactive bifunctional chelator. Since the conjugation of peptides on the liposomal surface has utilized the reaction of thiol with maleimide within 5 to 60 min at 25 °C (46-48), liposomal conjugation with a thiol-activable Cu-64-incorporated bifunctional chelator was considered to be a promising approach. Based on this aim, we proposed the scheme outlined in Figure 1.

The incorporation of Cu-64 to TETA-PDP was performed under mild conditions (30 °C) within an hour and the reaction progress could easily be confirmed by radio TLC (Rf 0.45 with 10% ammonium acetate and methanol (1:1, v/v)). However, the reaction progress of **4** could not be monitored by radio-TLC due to the similar retention factor (both Rf = 0) of ^{64}CuCl (**5**) and ^{64}Cu-CB-TE2A-PDEA (**6**). In addition, the stability of pyridine dithiol in CB-TE2A-PDEA (**4**) during chelation at 85 °C was a concern. Accordingly, the reaction progress was assessed by HPLC analysis (figure 2). Radio HPLC analysis demonstrated that the chelation of Cu-64 into CB-TE2A-PDEA (**4**) was completed within one hour and the conversion of **6** to thiol (**7**) succeeded without de-complexation of Cu-64 from the chelators or decomposition of **6** and **7** (figure 2).

Next we moved forward to the optimization of labeling yield, as outlined in figure 4. For this study, 1 mol% maleimide and 1 mol% maleimide-PEG2k liposomes were employed to compare the labeling efficiency and to determine whether the PEG2k brush decreases the conjugation (figure 3). In order to maintain 5 mol% PEG2k on the surface of the liposomes, which facilitates long circulation of liposomes in the blood pool, either 5 mol% DSPE-PEG2k-OMe or a combination of 4 mol% DSPE-PEG2k-OMe and 1 mol% DSPE-PEG2k maleimide were incorporated within our formulations (figure 3). The labeling study

(measured in four molar ratios of maleimide lipid versus TETA-PDP (**2**)) showed that at least an eight fold lower molar concentration of **2** should be incubated with both liposomes to obtain greater than 90% yield (pH 7, 40 min incubation) (figure 5). The BFC is fully accessible with similar labeling efficiency whether the maleimide sits under the PEG2k-brush or at the end of the PEG2k lipid.

In general, more than 6000 mCi/μmol maleimide lipids could be obtained from Cu-64 generated from a Ni-64 target (49) under the assumption of 100 percent chelation of Cu-64 with the BFC and 100% conjugation of ^{64}Cu-BFC to the maleimide lipid. However, due to the excess BFC (10 times more than Cu-64) and maleimide (7 times more than ^{64}Cu-BFC), the specific activity calculated from maleimide lipids was 20.8 mCi/μmol maleimide lipids. Preclinical studies of Doxil® (long circulating liposome) typically use 2.5-20 mg lipids/kg mouse for the treatment of tumor bearing mice (7). In our model, approximately 40 mg/kg lipids were administered for the Cu-64 labeled liposomal study and a high signal to noise ratio was achieved. The liposome dose can be reduced if imaging with Cu-64 labeled liposomes shows a tumor accumulation at a lower liposome dose, and particularly if the Cu-64 has a high effective specific activity (> 6000 mCi/μmol Cu-64) (49).

Previously, ^{99m}Tc-BMEDA encapsulated liposomes (50) and ^{99m}Tc-HYNIC surface labeled liposomes (26) have been considered as stable labeling methods for liposomal SPECT studies. For liposomal PET studies, our prior labeling method showed sufficient stability to represent liposomal behavior *in vivo* (36). In this connection, the second step of the study was to evaluate the liposomal stability *in vitro* and *in vivo* after the conjugation of different bifunctional chelators (**6** and **8**). The stability of 1 mol% maleimide-PEG2k liposomes was compared after the conjugation with ^{64}Cu-TETA-PDP and ^{64}Cu-CB-TE2A-PDEA to evaluate the effect of the chelator. Maleimide and maleimide-PEG2k liposomes were compared after labeling with ^{64}Cu-TETA-PDP to determine whether the conjugated ^{64}Cu-TETA-PDP is stable under a PEG2k brush or the end of a PEG2k lipopolymer. To answer those questions, the stability of three liposomal formulations (^{64}Cu-TETA, ^{64}Cu-TETA-PEG2k, and ^{64}Cu-CB-TE2A-PEG2k liposomes) was examined *in vitro* and *vivo*.

In vitro assays performed with ^{64}Cu-TETA, ^{64}Cu-TETA-PEG2k, and ^{64}Cu-CB-TE2A-PEG2k liposomes showed that 89%, 86%, and 86% radioactivity is still associated with the liposomal fraction, respectively, at 48 hours (figure 6). This result was similar to that obtained in our previous study (in which 88% of the radioactivity was in the liposomal fraction) (36). The radiochemical purity of each liposomal fraction determined with radio TLC was more than 98%.

A normal rat study performed by Bao et al. using ^{99m}Tc-BMEDA encapsulated-liposomes reported a two phase blood clearance of liposomes (50). Forty percent of activity remained in the blood pool at 18 hours based on the decay function in their study ($y = 36.4 \times e^{-0.315 \times t} + 63.7 \times e^{-0.0264 \times t}$, y = % activity in blood, t = time (h)). *S. aureus* infected rats studied by Laverman et al. using ^{99m}Tc-HYNIC surface-labeled liposomes yielded 40% of the initial blood-pool activity at 24 hours (27). In our study, the TAC data simulated with a one phase exponential decay showed that the 60% clearance times were 24 h (^{64}Cu-TETA liposomes), 24 h (^{64}Cu-TETA-PEG2k liposomes) and 21 h (^{64}Cu-CB-TE2A-PEG2k liposomes) (figure 8b). There was no significant difference in the time required for 60% clearance between ^{64}Cu-TETA liposomes and ^{64}Cu-TETA-PEG2k liposomes. Given the slow release and the anticipated reduction in Cu-64 transchelation with ceruloplasmin and superoxide dismutase (SOD) with CB-TE2A as the Cu-64 chelator, we had hypothesized that the accumulation of Cu-64 in the liver and spleen would be lower than that observed using TETA (51,52). The TAC obtained here illustrated that liver accumulation at 48 h ($P<0.001$) was higher for ^{64}Cu-CB-TE2A-PEG2k liposomes than for ^{64}Cu-TETA and ^{64}Cu-TETA-

PEG2k liposomes (figure 8c). The lipophilicity of ^{64}Cu-labeled CB-TE2A, and negative charge of ^{64}Cu-TETA may contribute to the comparatively larger RES accumulation of ^{64}Cu-CB-TE2A-PEG2k liposomes. Due to the slow clearance and high uptake of ^{64}Cu-CB-TE2A-PEG2k liposomes in the liver (figure 8c) and spleen (figure 8d), the decay-corrected whole body activity (^{64}Cu-CB-TE2A-PEG2k liposome) at 48 hours was also higher than other formulations (^{64}Cu-CB-TE2A-PEG2k liposomes vs ^{64}CuTETA liposomes, $p<0.001$; ^{64}Cu-CB-TE2A-PEG2k liposomes vs ^{64}Cu-TETA-PEG2k liposomes, $p<0.01$; figure 8a).

Similar to the TAC data, the liver ($P<0.001$) and spleen ($P<0.001$) biodistribution at 48 hours (table 1) showed that the properties of all three liposomal formulations differed , while a small but insignificant difference in accumulation was observed in the kidneys, lung, heart, blood, intestine and muscle. At 48 hours post-injection, liposomal accumulation of ^{64}Cu-TETA liposomes in the liver was 3.3 fold lower as compared with ^{64}Cu-CB-TE2A-PEG2k liposomes ($P<0.001$), and 2.2 times less than ^{64}Cu-TETA-PEG2k liposomes ($P<0.001$). Accumulation in the spleen also varied with ^{64}Cu-CB-TE2A-PEG2k liposomes > ^{64}Cu-TETA-PEG2k liposomes > ^{64}Cu-TETA liposomes (Table 1). According to the previous literature, ^{64}Cu-CB-TE2A showed lower uptake in the liver and higher resistance to transchelation than ^{64}Cu-TETA (51,52) but these reports involve the pharmacokinetics of chelators with (53) or without conjugation to a peptide (52). The comparison of ^{18}F-labeled RGD peptides with a PEG spacer ([^{18}F]FB-PEG-RGD) or without PEG ([^{18}F]FB-RGD), reported by Chen et. al, did not show a difference in accumulation of radioactivity in the liver although the blood clearance of [^{18}F]FB-PEG-RGD was slower than [^{18}F]FB-RGD (4,54). In contrast, the liver and spleen accumulation of [^{125}I]PEG-DPDPE was greater than [^{125}I]DPDPE (55). In (54), F-18 was labeled at the end of the PEG chain and, in (55), I-125 was labeled on the tyrosine residue between DPDPE and the PEG chain. Both results indicate that the presence of a PEG spacer is not necessarily correlated with the accumulation of radioactivity in the liver and spleen. The labeling position and molecular structure is also likely to affect the RES accumulation of activity. In our study, the radiolabel was at the end of the lipid or PEG.

The differences in liver radioactivity observed here between formulations may in part be due to the protective effect of the PEG2k spacer brush while liposomes are passing through the perisinusoidal space and sinusoids. In our previous liposomal study using 6-BAT-lipid with PEG1.2k as a spacer between the lipid and chelator, 6.21 ± 0.66 %ID/g remained in the liver and 13.61 ± 6.19 in the spleen at 48 hours (36); here, with ^{64}Cu-TETA liposomes, 6.88 ± 0.97 %ID/g remained in the liver and 12.26 ± 0.70 %ID/g in the spleen (Table 1). Those values are smaller than radioactivity in the liver and spleen resulting from both ^{64}Cu-TETA-PEG2k and ^{64}Cu-CB-TE2A-PEG2k liposomes (Table 1). ^{64}Cu-chelator complexes of 6-BAT liposomes (36) and ^{64}Cu-TETA liposomes are likely to be hidden under the PEG2k brush while ^{64}Cu-chelator complexes of ^{64}Cu-TETA-PEG2k liposomes and ^{64}Cu-CB-TE2A-PEG2k liposomes are exposed at the end of the PEG2k brush.

Verkade et. al. reported that hepatic processing and biliary secretion of liposome-associated phosphatidylcholine (PC) is predominantly determined by the degradation of PC in the liver (56). The degraded products are partially secreted into bile (56). The similar radioactivity in the duodenum and jejunum of mice administered with the three formulations may result in part from slow release of radioactivity from the liver through the bile duct. Radioactivity in the kidney was also similar for the three formulations at 48 hours irrespective of the presence of the PEG spacer and the specific chelator. Similarities in the size, primary lipid species and surface charge of the three formulations contributes to similarities in the accumulation of radioactivity.

In summary, we have synthesized two thiol-reactive bifunctional chelators, TETA-PDP and CB-TE2A-PDEA and developed a liposomal labeling method using maleimide lipid with those BFCs. An *in vitro* assay with mouse serum showed a similar liposomal stability for the three liposomal formulations. Liposomes labeled with the BFCs were stable in the blood pool over 48 hours and the 60% clearance time was 21 - 24 hours. The presence of the PEG spacer between the chelator and lipid did not significantly alter the labeling efficiency and the clearance rate of liposomes from the blood pool. The location of the ^{64}Cu-chelator complex influences the liposomal uptake in liver and spleen. The bifunctional chelator as a post-labeling method is applicable for liposomal labeling as well as labeling of antibodies and other nanoparticle formulations.

Acknowledgments

We thank the staff in the CMGI (Center for Molecular and Genomic Imaging, UC Davis) for handling ^{64}Cu and imaging studies. We appreciate the support of NIH R01 CA016861, R01 CA103828, and R01 CA134659, and NCI 5R01 CA93375.

Abbreviations

HSPC	hydrogenated soy *L*-*α*-phosphatidylcholine
DSPE	1,2-distearoyl-*sn*-glycero-3-phosphoethanolamine
DSPE-PEG2k-OMe	1,2-distearoyl-*sn*-glycero-3-phosphoethanolamine-*N*-[methoxy(polyethylene glycol)-2000]
MI	maleimide
HOBt	*N*-hydroxybenzotriazole
EDCI	(3-(dimethylamino)propyl)ethyl carbodiimide
DIPEA	diisopropylethylamine

LITERATURE CITED

1. Medina OP, Zhu Y, Kairemo K. Targeted liposomal drug delivery in cancer. Curr. Pharm. Des. 2004; 10:2981–2989. [PubMed: 15379663]
2. Torchilin VP. Recent advances with liposomes as pharmaceutical carriers. Nat. Rev. Drug Discovery. 2005; 4:145–160.
3. Andresen TL, Jensen SS, Jorgensen K. Advanced strategies in liposomal cancer therapy: Problems and prospects of active and tumor specific drug release. Prog. Lipid Res. 2005; 44:68–97. [PubMed: 15748655]
4. Klibanov AL, Maruyama K, Torchilin VP, Huang L. Amphipathic polyethyleneglycols effectively prolong the circulation time of liposomes. FEBS Lett. 1990; 268:235–237. [PubMed: 2384160]
5. O'Shaughnessy JA. Pegylated liposomal doxorubicin in the treatment of breast cancer. Clin Breast Cancer. 2003; 4:318–328. [PubMed: 14715106]
6. Torchilin VP, Omelyanenko VG, Papisov MI, Bogdanov AA Jr. Trubetskoy VS, Herron JN, Gentry CA. Poly(ethylene glycol) on the liposome surface: on the mechanism of polymer-coated liposome longevity. Biochim. Biophys. Acta. 1994; 1195:11–20. [PubMed: 7918551]
7. Gabizon A, Shmeeda H, Barenholz Y. Pharmacokinetics of pegylated liposomal Doxorubicin: review of animal and human studies. Clin. Pharmacokinet. 2003; 42:419–436. [PubMed: 12739982]
8. Barratt G, Legrand P. Comparison of the efficacy and pharmacology of formulations of amphotericin B used in treatment of leishmaniasis. Curr. Opin. Infect. Dis. 2005; 18:527–530. [PubMed: 16258327]

9. Lestini BJ, Sagnella SM, Xu Z, Shive MS, Richter NJ, Jayaseharan J, Case AJ, Kottke-Marchant K, Anderson JM, Marchant RE. Surface modification of liposomes for selective cell targeting in cardiovascular drug delivery. J. Controlled Release. 2002; 78:235–247.
10. Mamot C, Drummond DC, Greiser U, Hong K, Kirpotin DB, Marks JD, Park JW. Epidermal growth factor receptor (EGFR)-targeted immunoliposomes mediate specific and efficient drug delivery to EGFR- and EGFRvIII-overexpressing tumor cells. Cancer Res. 2003; 63:3154–3161. [PubMed: 12810643]
11. Park JW, Kirpotin DB, Hong K, Shalaby R, Shao Y, Nielsen UB, Marks JD, Papahadjopoulos D, Benz CC. Tumor targeting using anti-her2 immunoliposomes. J controlled Release. 2001; 74:95–113.
12. Lukyanov AN, Elbayoumi TA, Chakilam AR, Torchilin VP. Tumor-targeted liposomes: doxorubicin-loaded long-circulating liposomes modified with anti-cancer antibody. J. Controlled Release. 2004; 100:135–144.
13. Lu Y, Low PS. Folate-mediated delivery of macromolecular anticancer therapeutic agents. Adv. Drug Delivery Rev. 2002; 54:675–693.
14. Gabizon A, Shmeeda H, Horowitz AT, Zalipsky S. Tumor cell targeting of liposome-entrapped drugs with phospholipid-anchored folic acid-PEG conjugates. Adv. Drug Delivery Rev. 2004; 56:1177–1192.
15. Ferrara KW, Borden MA, Zhang H. Lipid-Shelled Vehicles: Engineering for Ultrasound Molecular Imaging and Drug Delivery. Acc. Chem. Res. 2009; 42:881–892. [PubMed: 19552457]
16. Schroeder A, Honen R, Turjeman K, Gabizon A, Kost J, Barenholz Y. Ultrasound triggered release of cisplatin from liposomes in murine tumors. J. Controlled Release. 2009; 137:63–68.
17. Wu GH, Milkhailovsky A, Khant HA, Fu C, Chiu W, Zasadzinski JA. Remotely triggered liposome release by near-infrared light absorption via hollow gold nanoshells. J. Am. Chem. Soc. 2008; 130:8175–8177. [PubMed: 18543914]
18. Mackanos MA, Larabi M, Shinde R, Simanovskii DM, Guccione S, Contag CH. Laser-induced disruption of systemically administered liposomes for targeted drug delivery. J. Biomed. Opt. 2009; 14:044009. [PubMed: 19725721]
19. Simoes S, Moreira JN, Fonseca C, Duzgunes N, de Lima MC. On the formulation of pH-sensitive liposomes with long circulation times. Adv. Drug Delivery Rev. 2004; 56:947–965.
20. Hamoudeh M, Kamleh MA, Diab R, Fessi H. Radionuclides delivery systems for nuclear imaging and radiotherapy of cancer. Adv. Drug Delivery Rev. 2008; 60:1329–1346.
21. Oku N. Delivery of contrast agents for positron emission tomography imaging by liposomes. Adv. Drug Delivery Rev. 1999; 37:53–61.
22. Phillips WT, Goins BA, Bao A. Radioactive liposomes. Wiley Interdiscip. Rev.: Nanomed. Nanobiotechnol. 2009; 1:69–83. [PubMed: 20049780]
23. Tilcock C, Ahkong QF, Fisher D. ^{99m}Tc-labeling of lipid vesicles containing the lipophilic chelator PE-DTTA: effect of tin-to-chelate ratio, chelate content and surface polymer on labeling efficiency and biodistribution behavior. Nucl. Med. Biol. 1994; 21:89–96. [PubMed: 9234269]
24. Ahkong QF, Tilcock C. Attachment of ^{99m}Tc to lipid vesicles containing the lipophilic chelate dipalmitoylphosphatidylethanolamine-DTTA. Int. J. Rad. Appl. Instrum. B. 1992; 19:831–840. [PubMed: 1428912]
25. Bao A, Goins B, Klipper R, Negrete G, Mahindaratne M, Phillips WT. A novel liposome radiolabeling method using ^{99m}Tc-“SNS/S” complexes: in vitro and in vivo evaluation. J. Pharm. Sci. 2003; 92:1893–1904. [PubMed: 12950007]
26. Phillips WT, Rudolph AS, Goins B, Timmons JH, Klipper R, Blumhardt R. A simple method for producing a technetium-99m-labeled liposome which is stable in vivo. Int. J. Rad. Appl. Instrum. B. 1992; 19:539–547. [PubMed: 1399684]
27. Laverman P, Dams ET, Oyen WJ, Storm G, Koenders EB, Prevost R, van der Meer JW, Corstens FH, Boerman OC. A novel method to label liposomes with ^{99m}Tc by the hydrazino nicotinyl derivative. J. Nucl. Med. 1999; 40:192–197. [PubMed: 9935076]
28. Gabizon A, Papahadjopoulos D. Liposome formulations with prolonged circulation time in blood and enhanced uptake by tumors. Proc. Natl. Acad. Sci. U. S. A. 1988; 85:6949–6953. [PubMed: 3413128]

29. Harrington KJ, Mohammadtaghi S, Uster PS, Glass D, Peters AM, Vile RG, Stewart JS. Effective targeting of solid tumors in patients with locally advanced cancers by radiolabeled pegylated liposomes. Clin. Cancer Res. 2001; 7:243–254. [PubMed: 11234875]
30. Hwang KJ, Merriam JE, Beaumier PL, Luk KF. Encapsulation, with high efficiency, of radioactive metal ions in liposomes. Biochim. Biophys. Acta. 1982; 716:101–109. [PubMed: 6807354]
31. Marik J, Tartis MS, Zhang H, Fung JY, Kheirolomoom A, Sutcliffe JL, Ferrara KW. Long-circulating liposomes radiolabeled with [^{18}F]fluorodipalmitin ([^{18}F]FDP). Nucl. Med. Biol. 2007; 34:165–171. [PubMed: 17307124]
32. Oku N, Tokudome Y, Tsukada H, Okada S. Real-time analysis of liposomal trafficking in tumor-bearing mice by use of positron emission tomography. Biochim. Biophys. Acta. 1995; 1238:86–90. [PubMed: 7654755]
33. Urakami T, Akai S, Katayama Y, Harada N, Tsukada H, Oku N. Novel amphiphilic probes for [^{18}F]-radiolabeling preformed liposomes and determination of liposomal trafficking by positron emission tomography. J. Med. Chem. 2007; 50:6454–6457. [PubMed: 18052025]
34. Mougin-Degraef M, Jestin E, Bruel D, Remaud-Le Saec P, Morandeau L, Faivre-Chauvet A, Barbet J. High-activity radio-iodine labeling of conventional and stealth liposomes. J. Liposome Res. 2006; 16:91–102. [PubMed: 16556552]
35. Awasthi V, Yee SH, Jerabek P, Goins B, Phillips WT. Cerebral oxygen delivery by liposome-encapsulated hemoglobin: a positron-emission tomographic evaluation in a rat model of hemorrhagic shock. J. Appl. Physiol. 2007; 103:28–38. [PubMed: 17615284]
36. Seo JW, Zhang H, Kukis DL, Meares CF, Ferrara KW. A novel method to label preformed liposomes with ^{64}Cu for positron emission tomography (PET) imaging. Bioconjugate Chem. 2008; 19:2577–2584.
37. Devaraj NK, Keliher EJ, Thurber GM, Nahrendorf M, Weissleder R. ^{18}F labeled nanoparticles for in vivo PET-CT imaging. Bioconjugate Chem. 2009; 20:397–401.
38. Wadas TJ, Wong EH, Weisman GR, Anderson CJ. Copper chelation chemistry and its role in copper radiopharmaceuticals. Curr. Pharm. Des. 2007; 13:3–16. [PubMed: 17266585]
39. Smith SV. Molecular imaging with copper-64. J. Inorg. Biochem. 2004; 98:1874–1901. [PubMed: 15522415]
40. Moran JK, Greiner DP, Meares CF. Improved synthesis of 6-[p-(bromoacetamido)benzyl]-1,4,8,11-tetraazacyclotetradecane- N,N′,N″,N″-tetraacetic acid and development of a thin-layer assay for thiol-reactive bifunctional chelating agents. Bioconjugate Chem. 1995; 6:296–301.
41. Moreau P, Tinkl M, Tsukazaki M, Bury PS, Griffen EJ, Snieckus V, Maharajh RB, Kwok CS, Somayaji VV, Peng Z, Sykes TR, Noujaim AA. Synthesis of the bifunctional chelating agent 6-(4-aminobenzyl)-1,4,8,11-tetra-azacyclotetradecane-*N*,*N*′,*N*″,*N* ‴-tetra acetic acid (H_2NBn-TETA). Synthesis. 1997:1010–1012.
42. Weisman GR, Wong EH, Hill DC, Rogers ME, Reed DP, Calabrese JC. Synthesis and transition-metal complexes of new cross-bridged tetraamine ligands. Chem. Commun. 1996:947–948.
43. Wong EH, Weisman GR, Hill DC, Reed DP, Rogers ME, Condon JS, Fagan MA, Calabrese JC, Lam KC, Guzei IA, Rheingold AL. Synthesis and characterization of cross-bridged cyclams and pendant-armed derivatives and structural studies of their copper(II) complexes. J. Am. Chem. Soc. 2000; 122:10561–10572.
44. Burns JA, Butler JC, Moran J, Whitesides GM. Selective reduction of Disulfides by tris(2-carboxyethyl)phosphine. J. Org. Chem. 1991; 56:2648–2650.
45. Han JC, Han GY. A procedure for quantitative determination of tris(2-carboxyethyl)phosphine, an odorless reducing agent more stable and effective than dithiothreitol. Anal. Biochem. 1994; 220:5–10. [PubMed: 7978256]
46. Frisch B, Boeckler C, Schuber F. Synthesis of short polyoxyethylene-based heterobifunctional cross-linking reagents. Application to the coupling of peptides to liposomes. Bioconjugate Chem. 1996; 7:180–186.
47. Roth A, Espuelas S, Thumann C, Frisch B, Schuber F. Synthesis of thiol-reactive lipopeptide adjuvants. Incorporation into liposomes and study of their mitogenic effect on mouse splenocytes. Bioconjugate Chem. 2004; 15:541–553.

48. Schelte P, Boeckler C, Frisch B, Schuber F. Differential reactivity of maleimide and bromoacetyl functions with thiols: Application to the preparation of liposomal diepitope constructs. Bioconjugate Chem. 2000; 11:118–123.

49. McCarthy DW, Shefer RE, Klinkowstein RE, Bass LA, Margeneau WH, Cutler CS, Anderson CJ, Welch MJ. Efficient production of high specific activity ^{64}Cu using a biomedical cyclotron. Nucl. Med. Biol. 1997; 24:35–43. [PubMed: 9080473]

50. Bao A, Goins B, Klipper R, Negrete G, Phillips WT. Direct ^{99m}Tc labeling of pegylated liposomal doxorubicin (Doxil) for pharmacokinetic and non-invasive imaging studies. J. Pharmacol. Exp. Ther. 2004; 308:419–425. [PubMed: 14610219]

51. Sun X, Wuest M, Weisman GR, Wong EH, Reed DP, Boswell CA, Motekaitis R, Martell AE, Welch MJ, Anderson CJ. Radiolabeling and in vivo behavior of copper-64-labeled cross-bridged cyclam ligands. J. Med. Chem. 2002; 45:469–477. [PubMed: 11784151]

52. Boswell CA, Sun X, Niu W, Weisman GR, Wong EH, Rheingold AL, Anderson CJ. Comparative in vivo stability of copper-64-labeled cross-bridged and conventional tetraazamacrocyclic complexes. J. Med. Chem. 2004; 47:1465–1474. [PubMed: 14998334]

53. Sprague JE, Peng Y, Sun X, Weisman GR, Wong EH, Achilefu S, Anderson CJ. Preparation and biological evaluation of copper-64-labeled tyr3-octreotate using a cross-bridged macrocyclic chelator. Clin. Cancer Res. 2004; 10:8674–8682. [PubMed: 15623652]

54. Chen X, Park R, Hou Y, Khankaldyyan V, Gonzales-Gomez I, Tohme M, Bading JR, Laug WE, Conti PS. MicroPET imaging of brain tumor angiogenesis with ^{18}F-labeled PEGylated RGD peptide. Eur. J. Nucl. Med. Mol. Imaging. 2004; 31:1081–1089. [PubMed: 15118844]

55. Witt KA, Huber JD, Egleton RD, Roberts MJ, Bentley MD, Guo L, Wei H, Yamamura HI, Davis TP. Pharmacodynamic and pharmacokinetic characterization of poly(ethylene glycol) conjugation to met-enkephalin analog [D-Pen2, D-Pen5]-enkephalin (DPDPE). J. Pharmacol. Exp. Ther. 2001; 298:848–856. [PubMed: 11454951]

56. Verkade HJ, Derksen JT, Gerding A, Scherphof GL, Vonk RJ, Kuipers F. Differential hepatic processing and biliary secretion of head-group and acyl chains of liposomal phosphatidylcholines. Biochem. J. 1991; 275:139–144. [PubMed: 2018469]

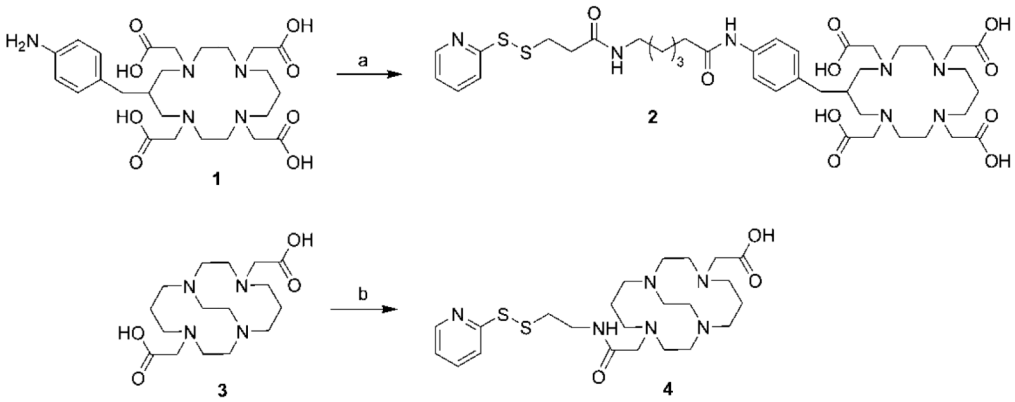

Scheme.

Synthesis of bifunctional chelators (BFCs) bearing TETA and CB-TE2A

Reagents. a) Sulfo-LC-SPDP (sulfosuccinimidyl-6-[3′(2-pyridyldithio)-propionamido] hexanoate), DI water, rt, 4 h. b) S-(2-aminoethyl)dithio-2-pyridine hydrochloride , HOBt, EDCI, DIPEA, DMF, rt, 6 h.

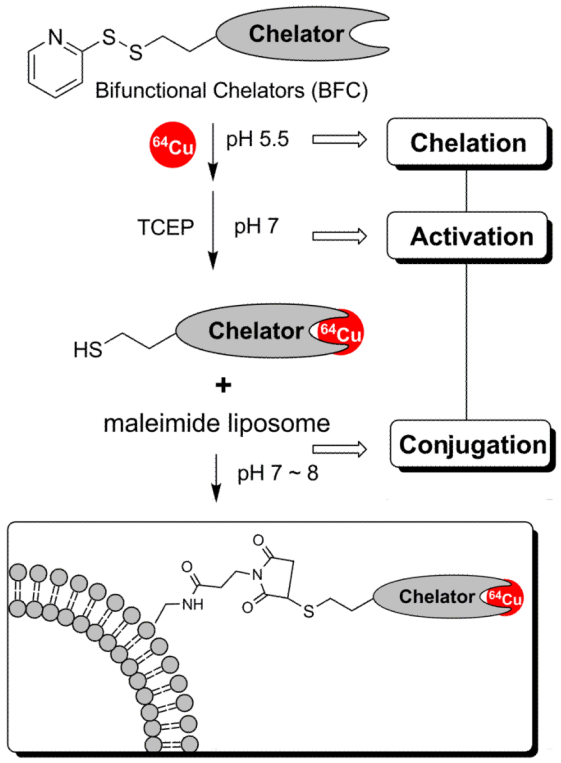

Figure 1.
General scheme of liposomal post-labeling with (BFC).

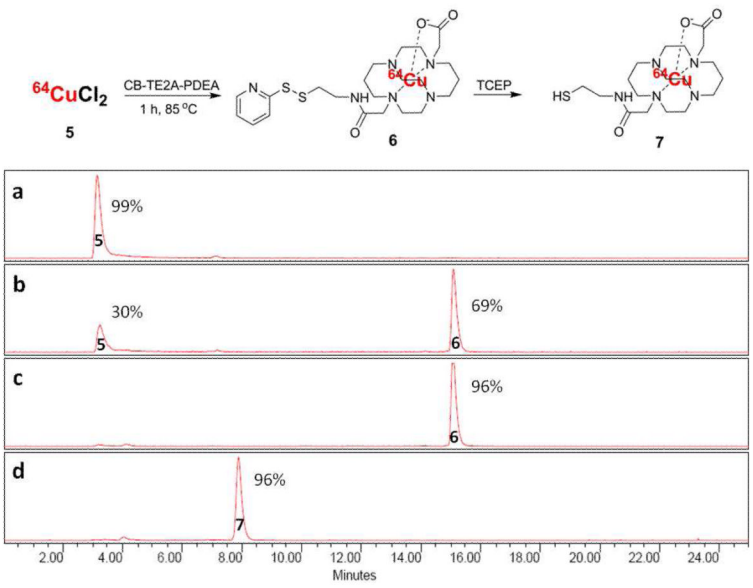

Figure 2.

HPLC radio chromatogram. (a) Immediately after mixing $^{64}CuCl_2$ and CB-TE2A-PDE at room temperature; (b) after 30 min incubation at 85 °C; (c) after 60 min incubation at 85 °C; (d) after addition of 10 equiv. of tris(2-carboxyethyl)phosphine (TCEP) at room temperature.

(a)

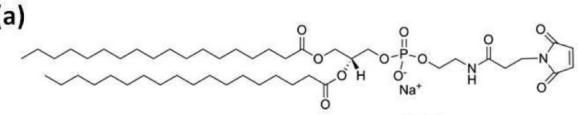

DSPE-maleimide **(a1)**

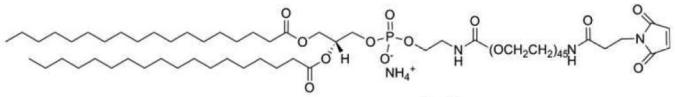

DSPE-PEG2k-maleimide **(a2)**

(b)

Liposomes	Formulation (mol%)			
	HSPC	DSPE-PEG2k-OMe	Chol[a]	Maleimide lipid
Long circulating liposome	56	5	39	-
1 mol% maleimide liposome	55	5	39	**1 (a1)**
1 mol% maleimide-PEG2k liposome	56	4	39	**1 (a2)**

Figure 3.

(a) Structure of maleimide lipids with and without PEG; (b) formulations of long circulating liposomes and modified formulations. Two different 1 mol% maleimide lipids were included.

[a]Cholesterol.

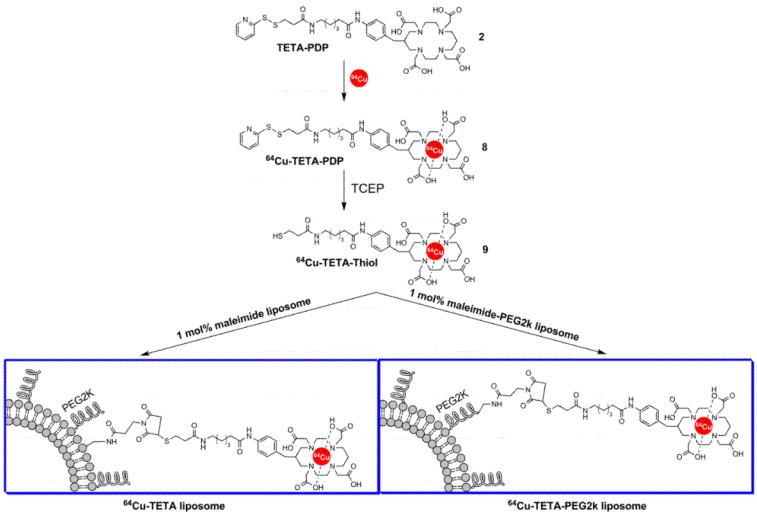

Figure 4.
Liposomal labeling model with ^{64}Cu-TETA-PDP and two maleimide liposomes.

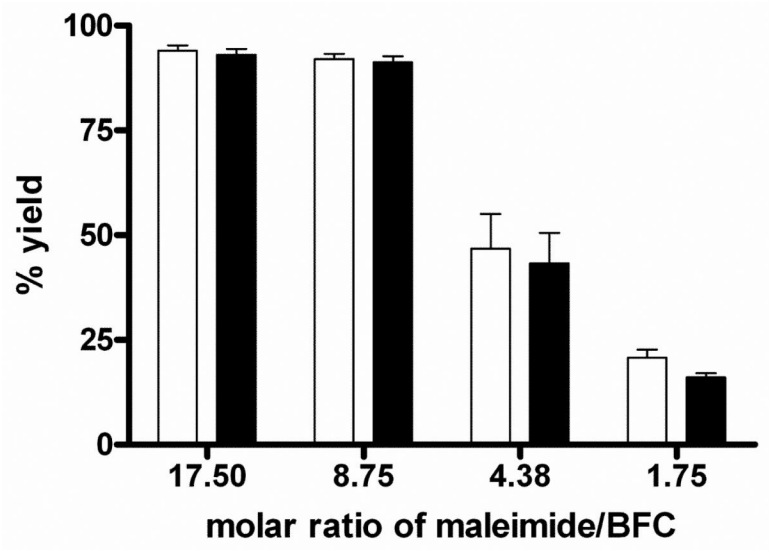

Figure 5.
Labeling yield (n = 4) of maleimide (1 mol%) liposomes with various molar ratios of Cu-64-incorporated TETA-BFC at pH 7 (black bar: 1 mol% maleimide liposomes, white bar: 1 mol % maleimide-PEG2k liposomes).

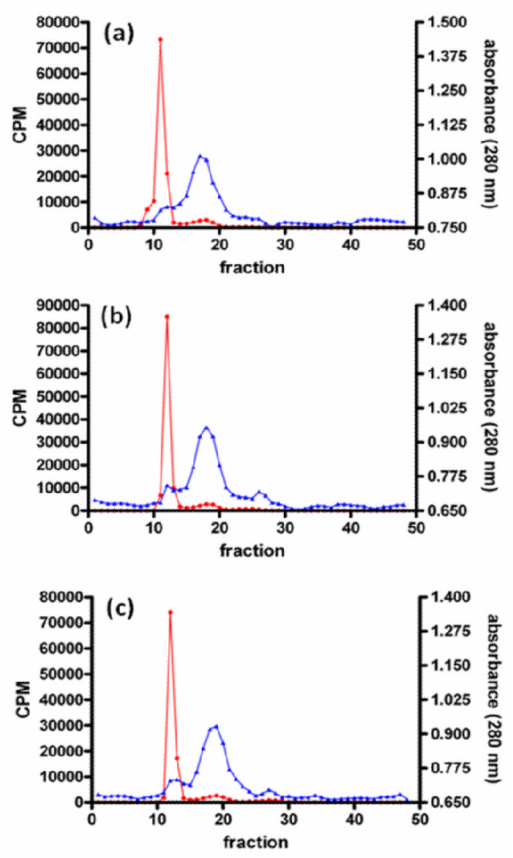

Figure 6.

In vitro assay of Cu-64-labeled maleimide liposomes. Chromatograms were obtained after 48 hour incubation in mouse serum and PBS (1:1, v/v) bearing (a) ^{64}Cu-TETA liposomes; (b) ^{64}Cu-TETA-PEG2k liposomes; and (c) ^{64}Cu-CB-TE2A- PEG2k liposomes. Red line represents radioactivity of liposomes detected by a gamma counter and blue line represents serum proteins detected by UV-absorbance at 280 nm.

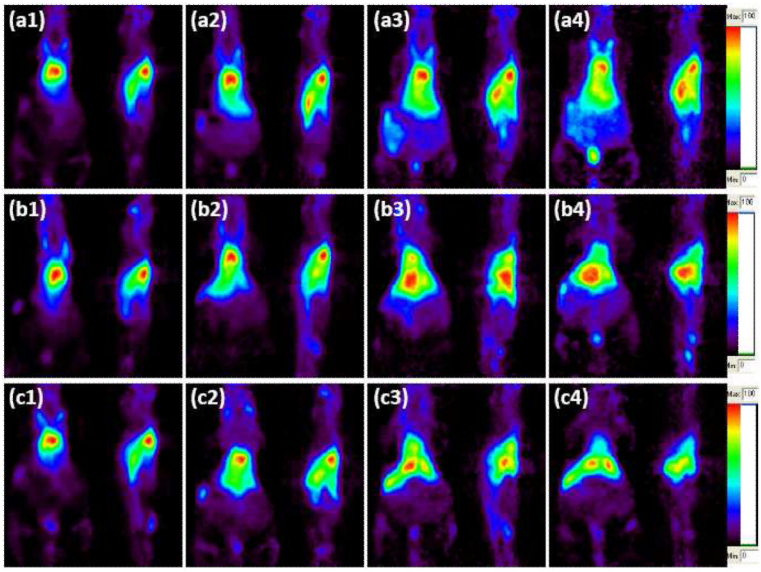

Figure 7.
Micro-PET images (left: coronal, right: sagittal) acquired after injection of ^{64}Cu-TETA liposomes (a1-4); ^{64}Cu-TETA-PEG2k liposomes (b1-4); and ^{64}Cu-CB-TE2A-PEG2k liposomes (c1-4) immediately after injection (a1-c1); 6 h later (a2-c2); 18 h later (a3-c3); and 28 h later (a4-c4). All images were acquired after reconstruction by filtered backprojection.

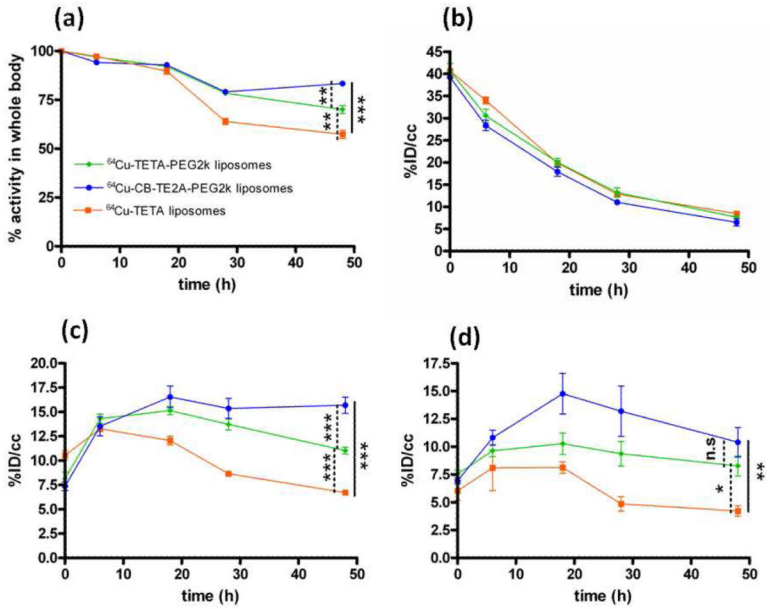

Figure 8.

(a) Whole body activity clearance (decay corrected). Time activity curves (TACs, %ID/cc) of heart (b), liver (c), and spleen (d) (n = 4 - 5) obtained from microPET by drawing regions of interest (ROI) after the injection of ^{64}Cu-TETA liposomes (orange square), ^{64}Cu-TETA-PEG2K liposomes (green diamond), and ^{64}Cu-CB-TE2A-PEG2k liposomes (blue round). ANOVA followed by Tukey's multiple comparison test was performed (error bars, mean ± STD; n.s., not significant; *$P < 0.05$; **$P < 0.01$; ***$P < 0.001$).

Table 1

Biodistribution of ^{64}Cu-TETA liposomes (n = 4), ^{64}Cu-TETA-PEG2K liposomes (n = 5), and ^{64}Cu-CB-TE2A-PEG2k liposomes (n = 4) in mice at 48 h after injection.

	^{64}Cu-TETA liposomes (n = 4)		**^{64}Cu-TETA -PEG2k liposomes (n = 5)**		**^{64}Cu-CB-TE2A-PEG2k liposomes (n = 4)**	
	%ID/g ± SD	**A**	**%ID/g ± SD**	**C**	**%ID/g ± SD**	**B**
Blood	8.71 ± 0.38	n.s.	8.35 ± 1.11	n.s.	6.85 ± 1.47	n.s.
Spleen	12.26 ± 0.70	*	20.25 ± 2.50	**	30.41 ± 1.40	***
Lungs	3.14 ± 0.25	n.s.	3.57 ± 0.20	**	2.24 ± 0.27	*
Diaphragm	1.28 ± 0.16	n.s.	1.41 ± 0.15	n.s.	1.18 ± 0.43	n.s.
Heart	2.89 ± 0.50	n.s.	3.34 ± 0.74	*	2.21 ± 0.40	n.s.
Liver	6.88 ± 0.97	**	15.15 ± 1.24	**	22.92 ± 1.94	***
Left kidney	6.14 ± 0.43	*	7.85 ± 1.17	*	5.80 ± 0.34	n.s.
Right kidney	6.03 ± 0.52	n.s.	7.60 ± 1.20	*	5.63 ± 0.33	n.s.
Duodenum	4.83 ± 0.57	n.s.	5.63 ± 0.14	n.s.	4.74 ± 0.23	n.s.
Jejunum	3.66 ± 0.63	n.s.	4.55 ± 0.61	*	2.79 ± 0.99	n.s.
Muscle	0.31 ± 0.06	n.s.	0.31 ± 0.09	n.s.	0.27 ± 0.03	n.s.

One-way analysis of variance followed by Tukey's multiple comparison test was performed. (A: ^{64}Cu-TETA liposomes vs ^{64}Cu-TETA -PEG2k liposomes; B: ^{64}Cu-TETA liposomes vs ^{64}Cu-CB-TE2A-PEG2k liposomes; C: ^{64}Cu-TETA -PEG2k liposomes vs ^{64}Cu-CB-TE2A-PEG2k liposomes, n.s., not significant

*$P < 0.05$

**$P < 0.01$

***$P < 0.001$)

Table 2

One phase exponential decay curves[a] of liposomal clearance from the blood pool in mice.

liposomes	$t_{1/2}$[b] (h)	span	k
^{64}Cu-TETA liposomes (n = 4)	18.22	41.10	0.03805
^{64}Cu-TETA- PEG2k liposomes (n = 5)	18.15	39.82	0.03819
^{64}Cu-CB-TE2A-PEG2k liposomes (n = 4)	16.20	38.32	0.04280

[a] Exponential decay curves were obtained from TAC of heart ($Y = span \times e^{-k \times t}$)

[b] Half clearance time